Thermodynamical constraints on the crystallization of a deep magma-ocean on Earth

Denis Andrault

C. R. Geoscience 351 (2019) 221–228

Contents lists available at ScienceDirect

Comptes Rendus Geoscience

www.sciencedirect.com

Internal Geophysics (Physics of Earth's Interior)

Thermodynamical constraints on the crystallization of a deep magma-ocean on Earth

Denis Andrault

Université Clermont Auvergne, CNRS, IRD, OPGC, Laboratoire Magmas et Volcans, 63000 Clermont-Ferrand, France

ARTICLE INFO

Article history:
Received 13 March 2018
Accepted after revision 7 June 2018
Available online 13 July 2018

Handled by Yanbin Wang

Keywords:
Magma ocean crystallization
Melting phase diagrams
Primordial core temperature

ABSTRACT

It has been argued that the crystallization of the magma ocean (MO) after the Moon-forming impact led to the formation of a basal magma ocean (BMO). We search which primordial conditions of pressure, temperature and chemical composition could be compatible with such scenario, based on thermodynamical constraints. The major requirement is an early formation of a viscous layer (VL) of mantle material (i.e. bridgmanite (Bg)) at mid lower-mantle depth, which could insulate thermally and chemically the BMO from the rest of the mantle. To produce such VL, Bg grains should be: (i) neutrally buoyant at mid lower-mantle depths, (ii) sufficiently abundant to produce an efficient insulating layer, and (iii) aggregated to the boundary layer from above and below. The first and the second require a large amount of MO crystallization, up to more than 45%, even in the most favorable case of all Fe partitioning into the melt. The latter is very questionable because the Bg grains have a very small settling velocity. We also investigate different scenarios of MO crystallization to provide constraints on the resulting core temperature. Starting from a fully molten Earth, a temperature as high as ~4725 K could be found at the core–mantle boundary (CMB), if the Bg grains settle early atop the CMB. Such a basal layer of Bg can efficiently decouple from each other the cooling rates of the core and the mantle above the VL. If the settling velocity of Bg grains is too low and/or the MO is too turbulent, such basal VL may not form. In this case, the CMB temperature after MO solidification should stabilize at ~4350 K. At this temperature, enough Bg grains are crystallized to make the mushy mantle viscous at any mantle depth.

1. Introduction

There exist two incompatible geodynamical models describing the crystallization of a deep MO in the primitive Earth. Thermodynamical constraints derived from recent experimental works provide new clues to discuss their viabilities. In a classical model, crystallization occurs from the bottom up and, upon cooling, the shallower mantle always presents a lower fraction of melt than below (Solomatov and Stevenson, 1993). An alternative model proposes the formation of a "primary" BMO (Labrosse et al., 2007). Such BMO appears when a solid shell of mantle material grows at mid-mantle depths, producing an early thermochemical separation between the upper and lower parts of the molten mantle (Fig. 1). A "secondary" type of BMO can also form. It would result from the downfall to the CMB of a relatively denser melt fraction (e.g., Boukare et al., 2015; Labrosse et al., 2015) or from the re-melting at the core vicinity of overturning dense cumulates (e.g., Elkins-Tanton et al., 2003). Even though both types of BMO result in the formation of a melt

E-mail addresses: denis.andrault@uca.fr, denis.andrault@gmail.com.

https://doi.org/10.1016/j.crte.2018.06.003

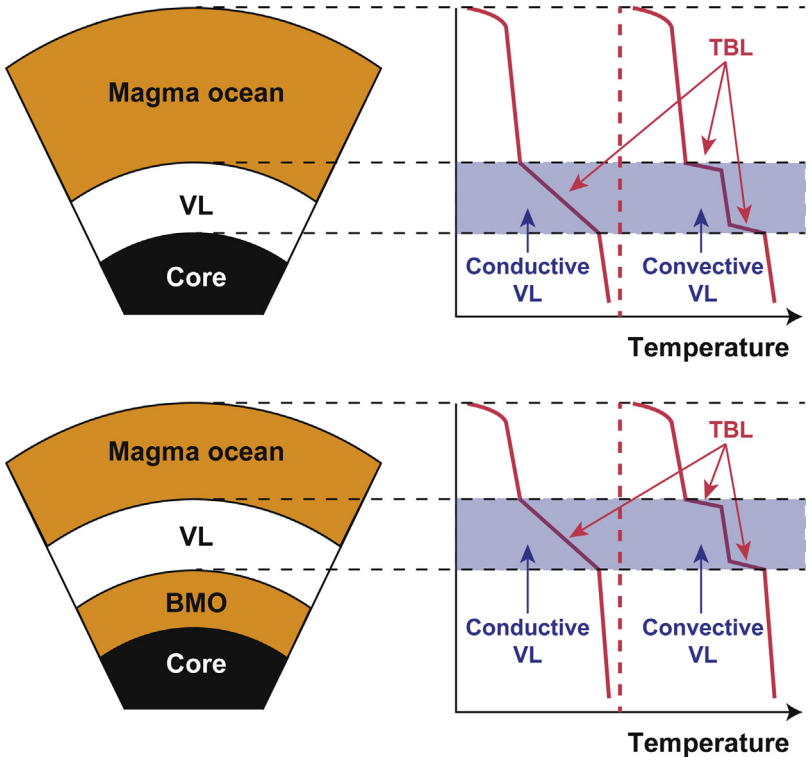

Fig. 1. Role of a viscous layer (VL; made of, e.g., bridgmanite) on the mantle geotherm (red lines). Both conductive and convective VL can sustain thermal boundary layer(s) (TBL), which decouple from each other the thermal states of the reservoirs located above and below the VL. The VL may form on the bottom (upper panels) or on the middle (lower panels) of the crystallizing magma ocean (MO).

layer atop the CMB, the two scenarios have radically different implications in terms of the early core temperature and BMO composition.

The classical model of MO crystallization is based on a degree of partial melting (F) decreasing with depth. This evolution arises when the P–T slope of the adiabatic temperature of the MO is flatter than the mantle melting curves (in particular that, but not only that one, of the liquidus). We argue below that the classical model can also operate for a liquidus profile presenting a strong curvature. This geodynamical model does not require chemical segregation between the different mantle reservoirs. Its initial thermal state (before an $n+1$ meteoritic impact) can already correspond to partial melting in the mantle, or not, depending on the accretion history. Then, the additional energy added to the mantle by a new impact increases the degree of partial melting (F) at mantle depths. Strong impacts can eventually yield mantle partial melting down to the CMB, for F_{CMB} values from 0 to 1. Thus, the classical model of MO crystallization can accommodate a very broad range of scenarios of Earth's accretion.

The alternative BMO model requires that the Moon-forming impact (MFI) yielded a major degree of mantle partial melting (F close to 1) at the CMB. The energy deposited during the MFI could very well be sufficient to melt the Earth entirely (Cuk and Stewart, 2012; Nakajima and Stevenson, 2015), however, there are geochemical measurements on the isotopes of tungsten (Mundl et al., 2017; Rizo et al., 2016) and, more controversially, on those of neodymium (Bouvier and Boyet, 2016), which strongly argue for the preservation of mantle reservoirs dating from the first ~50 million years of Earth history. This implies that either the MFI occurred before the closure of the isotopic systems or the Earth's mantle was not fully molten at the giant MFI. In this article, we only consider the hypothetical case for which the MFI has melted the Earth's mantle almost entirely (otherwise, the formation of a "primary" BMO cannot occur).

To conclude this introduction, we note that discussing the possible occurrence of a BMO in the primitive Earth is very different compared, for example, to the formation of the Moon. To explain the existence of the Moon, scientists have to find *the* right MFI, even if it is a very special one. It is needed to explain the observed Moon parameters such as its mass, orbital parameters, chemical composition, etc. In contrast, we do not *need* to adopt a scenario for BMO formation if it happens to be unconvincing. An extensive literature presents other possible explanations for the two major arguments raised in support of the primary BMO, which are: (i) the ultra-low velocity zones atop the CMB, and (ii) the persistence until today of the geodynamo.

2. The first step: Fast core cooling in the molten Earth

A concern of major importance related to the mechanism of MO crystallization is the primordial core temperature. It can help to constrain how much heat was stored in the core to participate in maintaining the geodynamo by

thermo-chemical convection over geological ages. It can also constrain the age of the inner core (e.g., Labrosse, 2015). Early on, the core–mantle segregation was contemporaneous with the presence of a MO on Earth, because a molten mantle favors largely the descent and the clustering of the small iron droplets (Rubie et al., 2015). Upon their descent toward the core, the Fe droplets can acquire thermal energy due to their own quasi-adiabatic compression and to the release of gravitational energy. After the droplets have aggregated in larger metallic ponds, the descent toward the core by the diapir mechanism tends to favor heat transfer to the viscous mantle (Monteux et al., 2009), while the channel mechanism favors a hotter core (Ke and Solomatov, 2009). It can yield a wide range of plausible thermal states for the primordial core. Still, it is generally accepted that the primordial core temperature was significantly higher than the mantle solidus, thus inducing some mantle melting at the CMB (Monteux et al., 2016), and possibly also above the mantle liquidus. In the latter case, the lowermost mantle was fully molten.

Melting of the mantle at the CMB can certainly induce a very high heat flux through the CMB, due to the low viscosity of silicate melts (Cochain et al., 2017), especially when the degree of partial melting is high. In the low-viscosity regime, thermal conductivity is dominated by thermal convection (Abe, 1997; Solomatov and Stevenson, 1993). At high Rayleigh numbers, the thermal boundary layers (TBL) are expected to be very thin, and a moderate temperature jump at the CMB is immediately translated into a major heat flux (Monteux et al., 2016). In the absence of a significant TBL, the adiabatic temperature gradient of the MO is expected to extend from the CMB to the Earth's surface (Fig. 2). Upon cooling, the amount of Bg grains increases, and a viscous transition eventually occurs at F values of 0.3–0.4, when the contact between solid grains becomes predominant (Abe, 1997; Scott and Kohlstedt, 2006). In the high-viscosity regime, the TBL become much larger, decreasing largely the heat flux at the CMB and enabling a larger temperature jump at the CMB (Fig. 1).

3. First crystallization of bridgmanite grains

The $(Mg,Fe)(Al,Si)O_3$ bridgmanite is the first mineral to appear upon MO crystallization at high mantle depth (Andrault et al., 2011; Fiquet et al., 2010; Ito and Katsura, 1992). Whatever was the true chemical composition of the primitive mantle between peridotite, pyrolite, or chondritic-type, the onset of crystallization can only occur at a temperature much lower than the melting curve of pure $MgSiO_3$-Bg. Reasons are: (i) the composition of Bg itself, which is $(Mg,Fe)(Al,Si)O_3$ instead of $MgSiO_3$, and (ii) the presence of two other minerals, the $CaSiO_3$-perovskite (CaPv) and the (Mg,Fe)O ferropericlase (Fp). In a previous article (Andrault et al., 2017), we examined the literature addressing the $MgSiO_3$-Bg melting curve (mostly *ab initio* calculation and shock wave experiments) and proposed to adopt the results from Stixrude and Karki, 2005, giving a melting temperature of ~5400 K at a CMB pressure of 135 GPa (Fig. 2). This temperature represents a far upper bound of the CMB temperature at the first crystallization of Bg grains in the MO on Earth. On this basis, we can state that whatever was the primordial core temperature at the CMB (possibly higher than 7500 K, Labrosse, 2015), the CMB cooled down rapidly far below 5400 K.

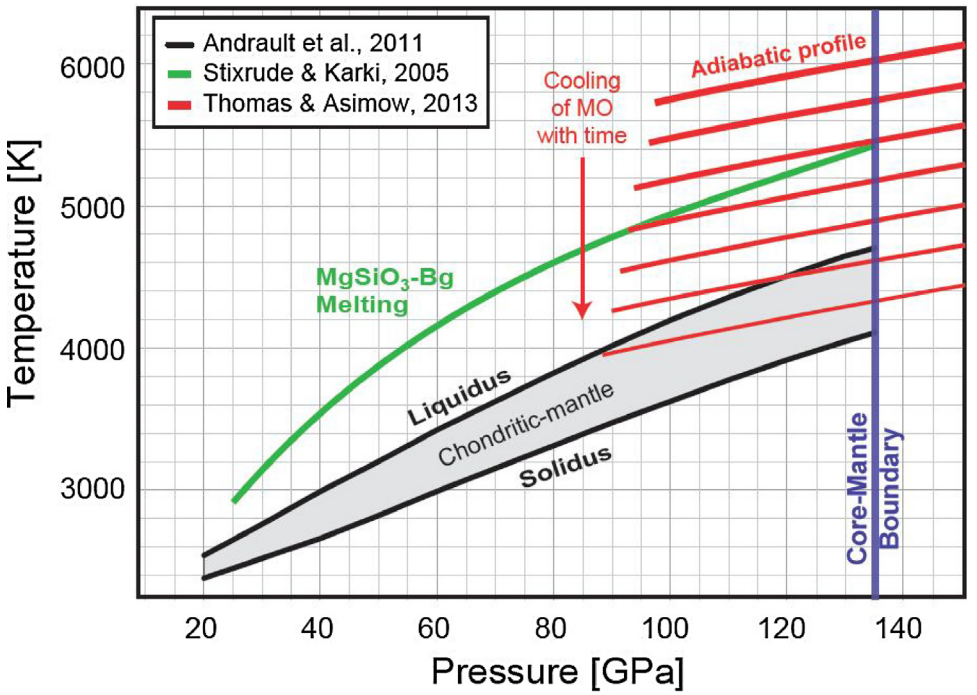

Fig. 2. Comparison between the melting curve of pure $MgSiO_3$-Bg (green line, Stixrude and Karki, 2005), the solidus and liquidus of a chondritic-type mantle (black lines, Andrault et al., 2011) and the adiabatic temperature profiles of the MO (red lines, Thomas and Asimow, 2013). We note that, despite remaining uncertainties about the liquidus profile of the deep mantle, it can only be significantly lower than the melting curve of pure $MgSiO_3$ bridgmanite.

In fact, the MO crystallization started when the mantle temperature became lower than the mantle liquidus at a given mantle depth. Above, the liquidus phase (Bg) is unstable (and thus dissolved) in the melt. The depth of first crystallization of Bg corresponds most likely to the CMB (Fig. 3A). However, it could also be a shallower depth if the liquidus profile presents a strong curvature at mid-lower mantle depths (Fiquet et al., 2010; Thomas et al., 2012) (Fig. 3E). This matter remains open to discussions due to large experimental uncertainties. In our previous work (Andrault et al., 2017), we show that the liquidus profile reported for peridotite (Fiquet et al., 2010) plots at same temperatures as the melting curve of pure $MgSiO_3$-Bg (Stixrude and Karki, 2005). Also, large Bg grains are observed at the center of the recovered samples. Both arguments suggest that the melting curve initially presented as the peridotite liquidus could instead be a measurement of the Bg melting curve. This leaves us with only one study reporting the liquidus curve for a chondritic-type, which is not an ideal situation because the liquidus profile is relatively difficult to determine using the laser heated diamond anvil cell. Still, the most likely situation is that the CMB temperature was ~4725 K at the onset of the Bg crystallization at the base of the mantle (Fig. 3A). This early CMB temperature would not be largely different if the liquidus profile would present a strong curvature (Fig. 3E).

Now, if the primitive mantle composition was depleted, or enriched, in SiO_2 (i.e. in Bg) compared to the chondritic-type mantle, this critical CMB temperature should be relatively lower, or higher, respectively, as suggested by the slope of the liquidus in the pseudo-binary melting diagram (Fig. 4). The maximum range of variation extends from ~4150 K, to a maximum of ~5400 K, for primordial-mantle compositions from that of pseudo-eutectic, to pure Bg, respectively.

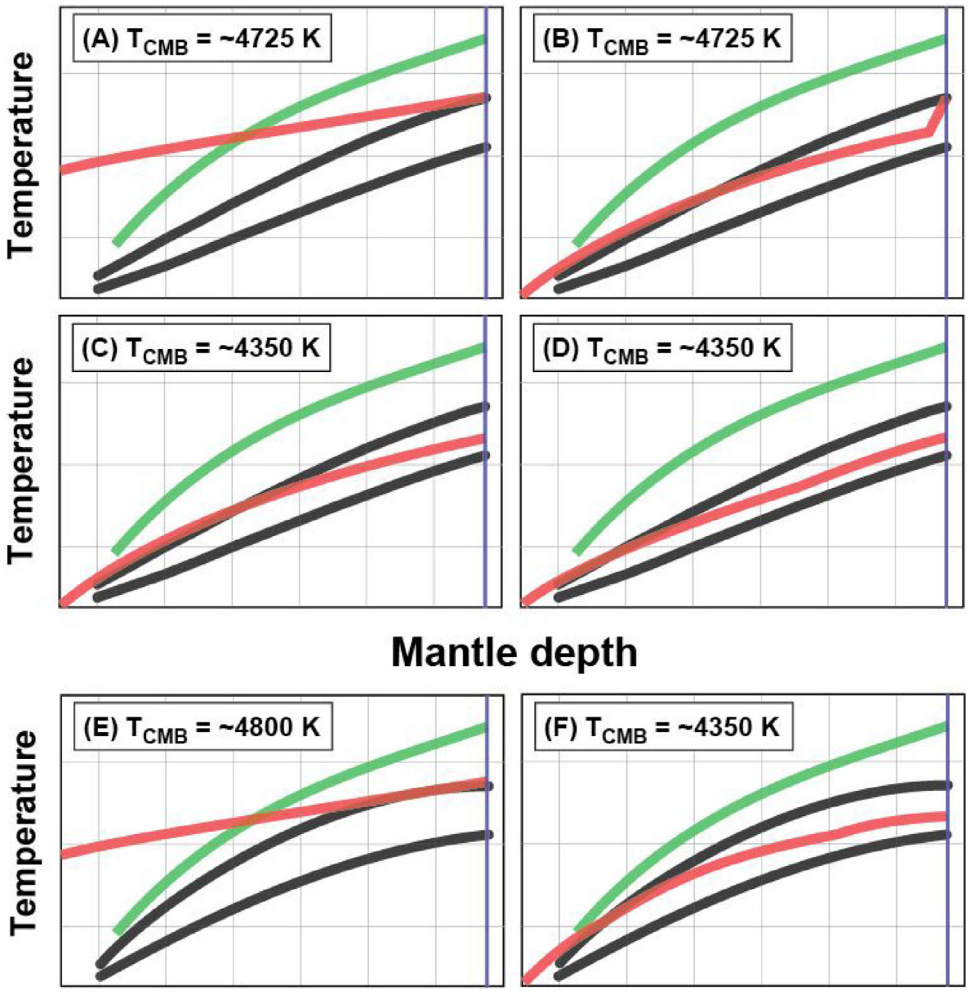

Fig. 3. Possible evolutions of the mantle thermal state along major events possibly occurring during MO crystallization after the MFI. [A, B, C, D] include a liquidus profile (upper black line) with a moderate curvature typical of a chondritic-type lower mantle (Andrault et al., 2011): [A] $(Mg,Fe)(Al,Si)O_3$ Bg starts to crystallize in a chondritic-type mantle composition, [B] A layer of Bg settles atop the CMB as soon as the MO starts to crystallize. Such Bg layer could host a relatively steep TBL. [C] An homogeneous chondritic-type mantle becomes viscous at the CMB (Monteux et al., 2016), [D] A sufficient amount of Bg (45 vol% of the lower mantle) is crystallized, which makes the Bg grains neutrally buoyant at mid lower-mantle depth (see Fig. 5). [E, F] include solidus and liquidus profiles with strong curvature: [E] is same as [A], [F] is same as [D].

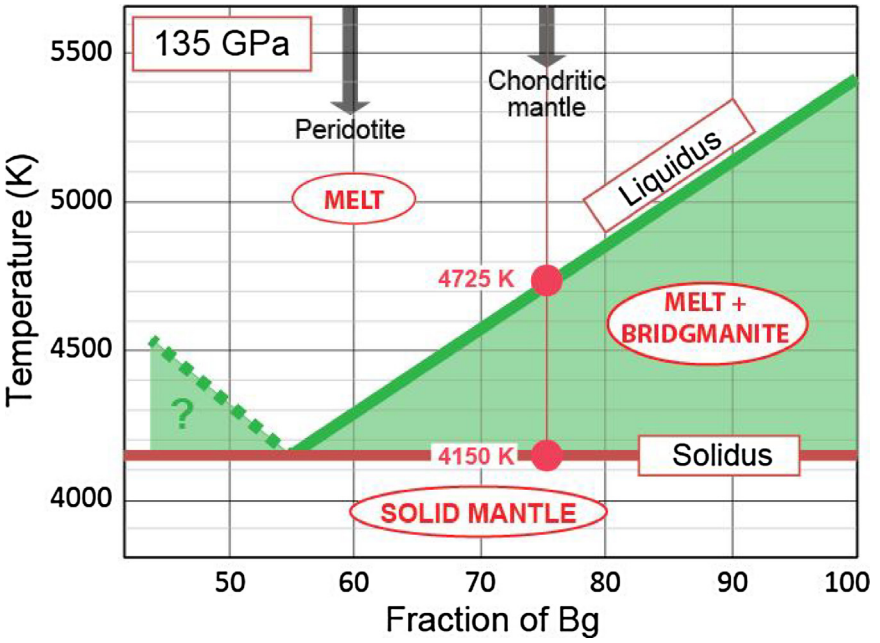

Fig. 4. Binary melting diagram at 135 GPa valid for a terrestrial mantle made of (Mg,Fe)(Al,Si)O_3 Bg, $CaSiO_3$-perovskite (CaPv) and (Mg,Fe)O ferropericlase (Fp) (modified from Fig. 4 of Andrault et al., 2017). The right end of the horizontal axis corresponds to Bg, the liquidus phase (e.g., Ito and Katsura, 1992). On the left is the mixture of CaPv and Fp; both phases are assumed to dissolve conjointly in the melt above the solidus temperature. The solidus and liquidus branches are drawn based on the melting point of pure Bg (5400 K, Stixrude and Karki, 2005), the mantle solidus (4150 K, Andrault et al., 2011; Fiquet et al., 2010) and liquidus (4725 K, Andrault et al., 2011) temperature for relevant mantle compositions and pseudo-eutectic melt compositions (Andrault et al., 2017; Tateno et al., 2014).

4. Requirements to achieve a viscous layer atop the CMB

It remains a long path between the crystallization of the first Bg grains to the formation of a VL of material enabling the thermochemical separation between the core, covered or not with the BMO, and the upper part of the MO (Fig. 1). As the first grains of Bg are denser than the melt in the MO (e.g., Andrault et al., 2017; Solomatov and Stevenson, 1993; Stixrude and Karki, 2005; Thomas and Asimow, 2013), they may form a Bg layer atop the CMB. We note that the mantle depth at which the Bg grains crystallize is not important, as long as they are not dissolved in the melt when they fall down to the CMB. A VL with a thickness of a few kilometers would be enough to host a TBL that would efficiently slow down core cooling (see Fig. 6 in Monteux et al., 2016). Consequently, if the chemical segregation is significant as early as at the onset of MO crystallization, the core temperature at the end of MO solidification would be close to the liquidus temperature at the CMB, i.e. ~4725 K (Fig. 3B). This is the maximum temperature that the core could logically achieve in the solid Earth, if the primordial MO composition is close to chondritic-type. For a mantle composition relatively enriched, or depleted, in SiO_2, then the maximum primordial core temperature would be higher, or lower, respectively.

Still, the efficiency of the sedimentation of Bg-grains in the crystallizing MO is questionable. For a Bg/melt density contrast of 1 to 3 percents (see Fig. 10 of Andrault et al., 2017), we estimate using the Stokes law that a spherical Bg-grain of 1 mm diameter would gravitationally settle at a velocity of 10^{-3} to $3{\cdot}10^{-3}$ m/s, considering a MO viscosity of 10^{-2} Pa·s (Cochain et al., 2017). Such value appears very small compared to the convective velocity in a turbulent MO reported at 10 m/s (Solomatov, 2000). In case the sedimentation of Bg grains would be inefficient, the formation of a TBL atop the CMB would be delayed, and the fast cooling of the core would not be slowed down at the critical temperature of ~4725 K. The occurrence of a VL would then occur when the viscous transition is achieved at the CMB after 60–70% of crystallization in a relatively homogeneous mantle (Monteux et al., 2016). Unfortunately, we do not have constraints on the evolution of the degree of partial melting F with temperature between the solidus and the liquidus. If we assume a linear dependence, then F values of 30–40% correspond to a primordial CMB temperature of ~4350 K (Fig. 3C).

5. Requirements to achieve a viscous layer at mid-mantle depth

To form a BMO, a layer of Bg should be neutrally buoyant at mid-lower-mantle depth. Bg grains can become neutrally buoyant after the MO crystallizes enough to increase sufficiently the Fe-content in the residual melt. We calculate the density contrast between Bg grains and the melt as a function of depth, of the degree of partial melting, and considering the Fe partition coefficient ($D_{Fe}^{Bg/Melt}$; unfortunately, the Mg–Fe exchange coefficient (K_{Fe-Mg}) is not well constrained experimentally) as an adjustable parameter because its value is controversially reported between 0.1 to 0.5 (Andrault et al., 2012; Nomura et al., 2011). Based on P–V–T equations of state of the solid

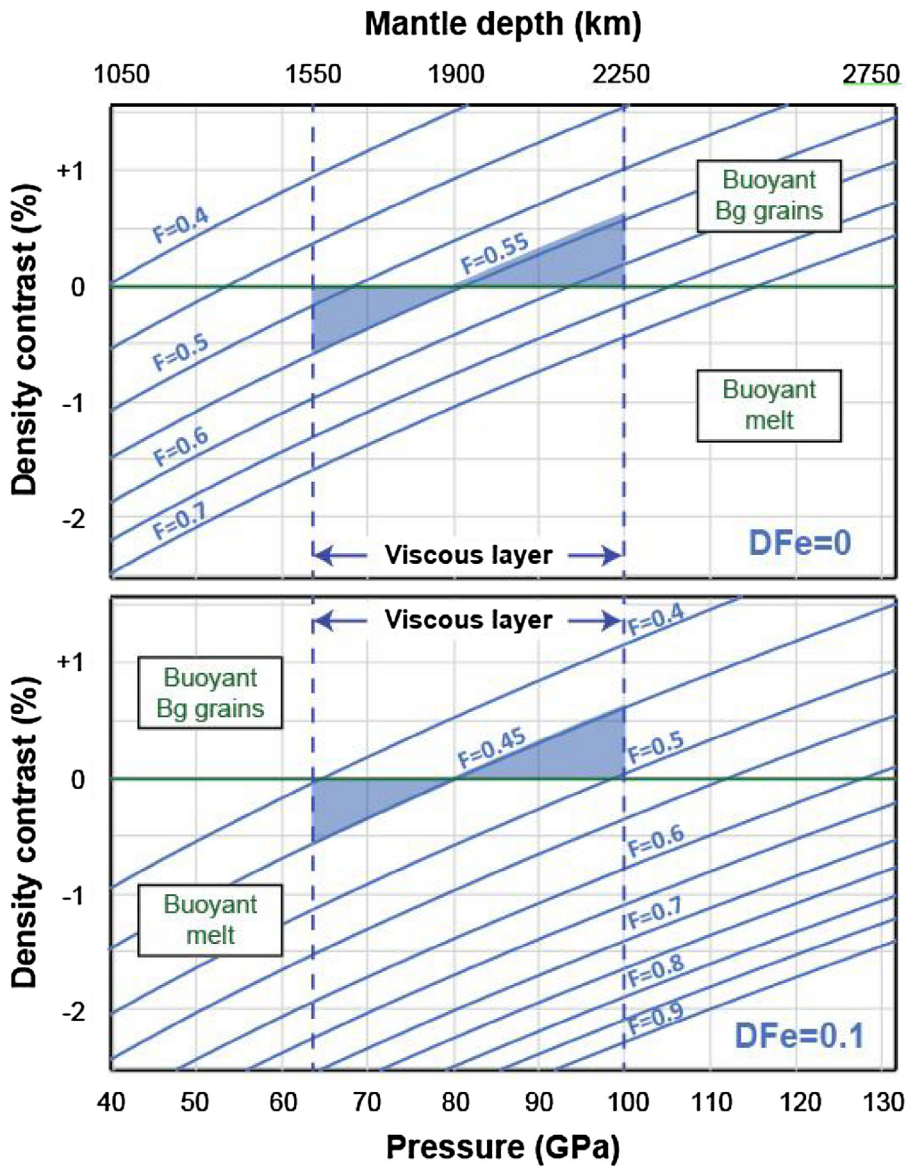

Fig. 5. Solid-melt density contrast in the context of a crystallizing magma ocean (modified from fig. 10 of Andrault et al., 2017). Upper and lower frames correspond to $D_{Fe}^{Bg/Melt}$ values of 0 (no Fe in Bg) and 0.1 (Nomura et al., 2011), respectively. For such low D_{Fe} values, Bg can become neutrally buoyant at a depth of 1900 km (~80 GPa) after 45 to 55% of the volume of the lower mantle is already crystallized (corresponding to F values from 0.55 to 0.45, respectively). In such cases, the maximum solid-melt density contrast at the upper and lower ends of an, e.g., 700-km viscous layer centered at a depth of 1900 km (i.e. at depths of 1550 and 2250 km) is significantly less than ~1%. In contrast, Bg never gets neutrally buoyant during the whole crystallization of the lower mantle if the $D_{Fe}^{Bg/Melt}$ value is 0.5 (Andrault et al., 2012).

phases, we first calculate the densities of Bg and of a solid assemblage made of a mixture Bg, CaPv and Fp with relative fractions corresponding to the melt's composition. Then, we apply to the melt a volume of fusion from 6 to 4% with increasing the pressure from 30 to 130 GPa, respectively, in order to retrieve the melt density (the procedure for density calculations is detailed in Andrault et al. (2017). The resulting constraints are the following: in order to make the Bg grains neutrally buoyant at pressures of 130 or 80 GPa, the volume of MO already crystallized should be (i) ~25–30% or ~45%, respectively, if Fe partitions exclusively to the melt (i.e. $D_{Fe}^{Bg/Melt} = 0$); (ii) ~40% or ~55%, respectively, if $D_{Fe}^{Bg/Melt} = 0.1$, as proposed in Nomura et al. (2011); (iii) more than 100% (i.e. no mathematical solution) if $D_{Fe}^{Bg/Melt} = 0.5$, as proposed in Andrault et al. (2012). In the latter case, the Bg grains always remain negatively buoyant during MO crystallization. Altogether, it appears that far more than 30% of MO crystallization is required to make the Bg grains neutrally buoyant in the deep lower mantle. This result is in good qualitative agreement with fig. 10 of Thomas et al. (2012).

The minimum value of 30 vol% of the lower mantle already crystallized corresponds to the volume of a shell of solid material 700 km in thickness sitting 500 km above

the CMB, in case all crystallized Bg grains would be aggregated to this layer. Such layer appears thinner than in the original drawing about the BMO (fig. 1 in Labrosse et al., 2007); however, it may be sufficient to insulate thermo-chemically a BMO from the shallower mantle. Nevertheless, to achieve 30 vol% of lower-mantle crystallization, or a still extreme but less critical assumption of 45 vol% (corresponding to 80 GPa and $D_{Fe}^{Bg/Melt} = 0$, see above), the MO temperature must be lowered to the point where the CMB temperature could have already reached the viscosity threshold at ~4350 K for a long time, if we assume a linear variation of F with temperature between the solidus and the liquidus (Figs. 3D and F). The situation is therefore ambiguous: when Bg grains eventually become neutrally buoyant at mid-mantle depth, a large shell of mantle material is already viscous atop the CMB. Such scenario does not correspond to the concept of "primary" BMO developed in Labrosse et al. (2007).

In addition, the formation of a solid shell at intermediate lower-mantle depths (the VL, which can host TBLs, see Fig. 1) requires the efficient aggregation of the crystallized Bg grains from above and below. In other terms, in addition to be neutrally buoyant at the center of the VL, the Bg grains should be negatively and positively buoyant above and below the VL, respectively. We estimate Bg-melt density contrasts smaller than 1% at depths of 1550 km (i.e. ~65 GPa) and 2250 km (i.e. ~100 GPa), if the Bg grains are neutrally buoyant at a depth of 1900 km (i.e. ~80 GPa) (Fig. 5). Using the same set of parameters as described above, such a small density contrast yields a maximum settling velocity of 10^{-3} m/s for the Bg grains in the MO above and below the VL. Consequently, the efficient aggregation of Bg grains to a VL at mid lower-mantle depth appears extremely questionable.

6. Core temperature at the CMB after MO solidification

If we consider that the settling of Bg grains to a VL (atop the CMB or at intermediate mantle depth) is poorly efficient in a highly turbulent MO (Solomatov and Stevenson, 1993), the core temperature after the MO solidification should be around 4350 K. This value is obtained under both assumptions of: (i) the first occurrence of a viscous (mushy) mantle atop the CMB (Fig. 3C) and (ii) the time when Bg grains become neutrally buoyant at mid-mantle depth (Figs. 3D and 5). Both situations correspond to a starting point after which the thermal states of the mantle and the core can evolve independently from each other (Fig. 1). The early sedimentation of a thin layer of Bg atop the CMB could potentially stabilize the core at a temperature up to that of the liquidus at ~4725 K (Fig. 3B).

The values of ~4350 K and ~4725 K would not be highly different if the liquidus profile were showing a large curvature as a function of depth (Fig. 3). However, we should point out that these values of ~4350 K and ~4725 K have large uncertainties. A first source of uncertainty is the difficulty to determine the liquidus temperatures using the diamond anvil cell coupled with laser heating. Other major parameters that would change these temperature values are: (i) a highly non-chondritic composition for the deep mantle at the time of the onset of MO crystallization, because the liquidus temperature would be different (Fig. 4) and (ii) a non-linear evolution of F between the solidus and the liquidus profiles, because it would change the temperature at which the viscous transition occurs in the mantle. Still, in all cases, core temperatures at the CMB higher than ~5000 K after the solidification of the MO appear incompatible with the thermodynamical constraints.

7. Possible occurrence of a secondary BMO

Previous works suggest that there could be mantle overturns early in the Earth history (Ballmer et al., 2017; Boukare et al., 2015; Elkins-Tanton et al., 2003; Labrosse et al., 2015) that could have contributed to the formation of secondary BMO. This topic is beyond the scope of this article; however, based on our analysis of relevant melting diagrams, we found that the melting behavior is pseudo-eutectic, such that a large degree of melt is generated within a very small temperature range above the solidus (Andrault et al., 2017). In such case, a very small fraction of melt highly enriched in Fe may not occur on the course of MO crystallization, due to a final bulk crystallization of a significant fraction of the MO. Still, early overturns related to surface processes and/or chemical reaction with the core may still produce a layer of dense melt atop the CMB. It remains that such mantle overturns are expected to occur at the latest steps of MO crystallization, when the thermal state of the deep Earth, including the core (Monteux et al., 2016), is already established.

Acknowledgments

I thank P. Asimow and an anonymous reviewer for their constructive comments. This research was financed by the French Government's Laboratory of Excellence Initiative No. ANR-10-LABX-0006, the "Région Auvergne", and the European Regional Development Fund. This is Laboratory of Excellence ClerVolc contribution No. 304.

References

Abe, Y., 1997. Thermal and chemical evolution of the terrestrial magma ocean. Phys. Earth Planet. Inter. 100, 27–39.
Andrault, D., Bolfan-Casanova, N., Bouhifd, M.A., Boujibar, A., Garbarino, Manthilake, G., Mezouar, M., Monteux, J., Parisiades, P., Pesce, G., 2017. Toward a coherent model for the melting behavior of the deep Earth's mantle. Phys. Earth Planet. Inter. 265, 67–81.
Andrault, D., Bolfan-Casanova, N., Lo Nigro, G., Bouhifd, M.A., Garbarino, G., Mezouar, M., 2011. Melting curve of the deep mantle applied to properties of early magma ocean and actual core–mantle boundary. Earth Planet. Sci. Lett. 304, 251–259.
Andrault, D., Petitgirard, S., Lo Nigro, G., Devidal, J.-L., Veronesi, G., Garbarino, G., Mezouar, M., 2012. Solid-liquid iron partitioning in Earth's deep mantle. Nature 487, 354–357.
Ballmer, M.D., Lourenco, D.L., Hirose, K., Caracas, R., Nomura, R., 2017. Reconciling magma-ocean crystallization models with the present-day structure of the Earth's mantle. Geochem. Geophys. Geosyst. 18, 2785–2806.
Boukare, C.E., Ricard, Y., Fiquet, G., 2015. Thermodynamics of the MgO–FeO–SiO_2 system up to 140 GPa: Application to the crystallization of Earth's magma ocean. J. Geophys. Res. Solid Earth 120, 6085–6101.
Bouvier, A.M., Boyet, M., 2016. Primitive Solar System materials and Earth share a common initial ^{142}Nd abundance. Nature 537, 399.

Cochain, B., Sanloup, C., Leroy, C., Kono, Y., 2017. Viscosity of mafic magmas at high pressures. Geophys. Res. Lett. 44, 818–826.
Cuk, M., Stewart, S.T., 2012. Making the moon from a fast-spinning earth: a giant impact followed by resonant despinning. Science 338, 1047–1052.
Elkins-Tanton, L.T., Parmentier, E.M., Hess, P.C., 2003. Magma ocean fractional crystallization and cumulate overturn in terrestrial planets: Implications for Mars. Meteorit. Planet. Sci 38, 1753–1771.
Fiquet, G., Auzende, A.L., Siebert, J., Corgne, A., Bureau, H., Ozawa, H., Garbarino, G., 2010. Melting of Peridotite to 140 Gigapascals. Science 329, 1516–1518.
Ito, E., Katsura, T., 1992. Melting of ferromagnesian silicates under lower mantle conditions. In: Syono, Y., Manghnani, M.H. (Eds.), High-Pressure Research: Application to Earth and Planetary Sciences. Terra Scientific Pub, Tokyo, pp. 315–322.
Ke, Y., Solomatov, V.S., 2009. Coupled core–mantle thermal evolution of early Mars. J. Geophys. Res.: Planets 114, E07004.
Labrosse, S., 2015. Thermal evolution of the core with a high thermal conductivity. Phys. Earth Planet. Inter. 247, 36–55.
Labrosse, S., Hernlund John, W., Hirose, K., 2015. Fractional Melting and Freezing in the Deep Mantle and Implications for the Formation of a Basal Magma Ocean. AGU Geophysical Monograph.
Labrosse, S., Hernlund, J.W., Coltice, N., 2007. A crystallizing dense magma ocean at the base of the Earth's mantle. Nature 450, 866–869.
Monteux, J., Andrault, D., Samiel, H., 2016. On the cooling of a deep terestrial magma ocean. Earth Planet. Sci. Lett. 448, 140–149.
Monteux, J., Ricard, Y., Coltice, N., Dubuffet, F., Ulvrova, M., 2009. A model of metal-silicate separation on growing planets. Earth Planet. Sci. Lett. 287, 353–362.
Mundl, A., Touboul, M., Jackson, M.G., Day, J.M.D., Kurz, M.D., Lekic, V., Helz, R.T., Walker, R.J., 2017. Tungsten-182 heterogeneity in modern ocean island basalts. Science 356 (2017), 66.
Nakajima, M., Stevenson, D.J., 2015. Melting and mixing states of the Earth's mantle after the Moon-forming impact. Earth Planet. Sci. Lett. 427, 286–295.
Nomura, R., Ozawa, H., Tateno, S., Hirose, K., Hernlund, J.W., Muto, S., Ishii, H., Hiraoka, N., 2011. Spin crossover and iron-rich silicate melt in the Earth's deep mantle. Nature 473, 199–202.
Rizo, H., Walker, R.J., Carlson, R.W., Horan, M.F., Mukhopadhyay, S., Manthos, V., Francis, D., Jackson, M.G., 2016. Preservation of Earth-forming events in the tungsten isotopic composition of modern flood basalts. Science 352, 809.
Rubie, D.C., Jacobson, S.A., Morbidelli, A., O'Brien, D.P., Young, E.D., de Vries, J., Nimmo, F., Palme, H., Frost, D.J., 2015. Accretion and differentiation of the terrestrial planets with implications for the compositions of early-formed Solar System bodies and accretion of water. Icarus 248, 89–108.
Scott, T., Kohlstedt, D.L., 2006. The effect of large melt fraction on the deformation behavior of peridotite. Earth Planet. Sci. Lett. 246, 177–187.
Solomatov, V.S., 2000. Fluid dynamics of terrestrial magma ocean. In: Canup, R.M., Righter, K. (Eds.), Origin of the Earth and Moon. The University of Arizona Press, Tucson, AZ, USA, pp. 323–338.
Solomatov, V.S., Stevenson, D.J., 1993. Nonfractional crystallization of a terrestrial magma ocean. J. Geophys. Res. 98, 5391–5406.
Stixrude, L., Karki, B.B., 2005. Structure and freezing of $MgSiO_3$ liquid in the Earth's lower mantle. Science 310, 297–299.
Tateno, S., Hirose, K., Ohishi, Y., 2014. Melting experiments on peridotite to lowermost mantle conditions. J. Geophys. Res. Solid Earth 119, 4684–4694.
Thomas, C.W., Asimow, P.D., 2013. Direct shock compression experiments on premolten forsterite and progress toward a consistent high-pressure equation of state for $CaO–MgO–Al_2O_3–SiO_2–FeO$ liquids. J. Geophys. Res. Solid Earth 118, 5738–5752.
Thomas, C.W., Liu, Q., Agee, C.B., Asimow, P.D., Lange, R.A., 2012. Multi-technique equation of state for Fe_2SiO_4 melt and the density of Fe-bearing silicate melts from 0 to 161 GPa. J. Geophys. Res. Solid Earth 117, B10206.